# Hydroclimatic Regime Shifts and Compound Heat–Dry Events in Rajshahi Division, Bangladesh: Integrating Thermal Gradients, Change-Point Detection, and Heat-Driven Dryness Dynamics (1992–2022)

**Md. Iqbal Hossain [a]**

a. Department of Urban and Regional Planning, Pabna University of Science and Technology, Pabna-6600, Rajshahi, Bangladesh.

**Corresponding author:*

Phone: +8801855708968 Email: hossain.iqbalrahi@gmail.com (Md. Iqbal Hossain)

**Acknowledgement**

The authors would like to express their sincere gratitude to all institutions and individuals who supported the completion of this research. We are especially thankful to Dr. Md. Kamrul Hasan for his valuable teaching on research methodology, academic inspiration, and continuous encouragement throughout the study. His guidance greatly contributed to the conceptual and analytical development of this research.

We also extend our appreciation to Md. Sumon Bappy, Research Assistant at Jahangirnagar University, for his constructive suggestions, technical support, and assistance during different stages of data analysis and manuscript preparation. Finally, the authors acknowledge the Bangladesh Bureau of Statistics and the Bangladesh Power Development Board for providing the statistical data used in this study.

**Authorship contribution statement**

**Md. Iqbal Hossain**: conceptualization, methodology, formal analysis, discussion, writing - original draft, writing - review & editing, data collection, data formatting & cleaning, Validation.

**Declaration of competing interest**

The authors declare that they have no known financial or interpersonal conflicts that could have affected the findings of this study.

**Ethics statement**

The Chairman of Pabna University of Science and Technology's Department of Urban and Regional Planning (Ethics Committee) granted ethics approval. The participants gave their informed agreement to take part in the study as well.

**Preprint Status Statement**

This is a non-peer-reviewed preprint submitted to EarthArXiv. This manuscript has not been submitted to any journal for peer review at this time.

**MD. IQBAL HOSSAIN**

# Hydroclimatic Regime Shifts and Compound Heat–Dry Events in Rajshahi Division, Bangladesh: Integrating Thermal Gradients, Change-Point Detection, and Heat-Driven Dryness Dynamics (1992–2022).


## Abstract

Hydroclimatic variability and compound climate extremes are increasingly affecting monsoon-dominated regions of South Asia, particularly drought-prone northwestern Bangladesh. However, integrated assessments of thermal dynamics, atmospheric moisture, land–atmosphere coupling, and compound heat–dry events remain limited in the regional context. Therefore, this study investigated long-term hydroclimatic changes and emerging heat-driven dryness conditions in Rajshahi Division during 1992–2022. Monthly hydroclimatic data, including air temperature, Earth skin temperature, specific humidity, and precipitation, were obtained from the NASA POWER database for eight districts of the division. Mann–Kendall trend analysis, Sen's slope estimator, Surface–Air Temperature Gradient (SATG), Heat-Driven Dryness Index (HDDI), compound event analysis, Pettitt change-point detection, and spatial vulnerability assessment were applied to evaluate regional hydroclimatic behavior. The results revealed significant decreases in air temperature and Earth skin temperature, while humidity and precipitation increased across both annual and seasonal scales. SATG exhibited persistent declining trends, indicating weakening land–atmosphere thermal coupling and reduced surface thermal contrast. HDDI values shifted from predominantly positive conditions during the early 1990s to increasingly negative conditions after the late 1990s, reflecting reduced heat-driven dryness and enhanced moisture availability. Compound heat–dry event frequency also declined substantially after the late 1990s, and Pettitt analysis identified significant hydroclimatic regime shifts during this transition period. Spatial assessment further revealed strong district-level variability, with Nawabganj showing the highest vulnerability conditions. Overall, the study demonstrates a gradual hydroclimatic transition from heat-dry dominance toward increasingly moisture-influenced conditions in northwestern Bangladesh. The findings provide an integrated framework for regional drought monitoring, climate adaptation planning, and future hydroclimatic research under changing monsoon conditions.



***Keywords*:** Hydroclimatic variability; Compound heat–dry events; Surface–Air Temperature Gradient (SATG); Heat-Driven Dryness Index (HDDI); Change-point detection; Rajshahi Division; Bangladesh; Land–atmosphere coupling.

# 1.Introduction

Climate change is increasingly altering global hydroclimatic systems through changes in temperature, precipitation, atmospheric moisture, and land–surface energy exchange. Many regions of the world are now experiencing stronger climate variability, irregular rainfall patterns, prolonged droughts, and more frequent extreme events(WMO, 2026). Rising global temperature enhances evaporation and atmospheric water demand(Karimzadeh et al., 2025), which directly affects regional water balance and ecosystem stability. Recent studies also indicate that hydroclimatic processes are becoming more interconnected under climate change conditions(Frédéric Talbot et al., 2025). As a result, understanding the combined behavior of thermal and moisture variables has become an important issue in climate science. Traditional single-variable climate assessments often fail to explain the complexity of evolving hydroclimatic systems(Apoorva Bamal et al., 2025). Therefore, integrated hydroclimatic analysis has received growing attention for understanding regional climate transitions and environmental stress.

South Asia is considered one of the most climate-sensitive regions because of its dependence on monsoon circulation, agricultural economy, and high population density(IWMI, 2026; Saira, 2023). Countries such as India, Pakistan, and Nepal have experienced increasing drought frequency, irregular monsoon rainfall, and severe heat stress during recent decades. Several studies reported that compound climate extremes, especially simultaneous heat and dryness conditions, are increasing across the region(Zhou et al., 2024). These compound events are more dangerous than isolated climate hazards because they intensify evapotranspiration, reduce soil moisture, and increase agricultural and environmental stress. Heat–dry interactions also create positive feedback mechanisms between land heating and atmospheric moisture deficit. Under dry surface conditions, sensible heat flux increases while evaporative cooling decreases(Karinou et al., 2025), which further intensifies surface warming. Consequently, compound heat–dry events are now recognized as an important indicator of hydroclimatic instability in monsoon-dominated regions.

Bangladesh also experiences strong hydroclimatic variability due to its tropical monsoon climate. Although the country generally receives high annual rainfall, large seasonal and spatial differences exist in temperature and precipitation distribution(M. R. Islam, 2019). Northwestern Bangladesh, particularly Rajshahi Division, is widely recognized as one of the hottest and driest regions of the country(Miah et al., 2022). The region frequently experiences high summer temperature, seasonal drought, groundwater stress, and irregular rainfall conditions. Much of the area overlaps with the Barind Tract, where low soil moisture retention(Ferozur et al., 2019) and limited groundwater recharge intensify hydroclimatic vulnerability(Sarker, T. & S., 2026). During recent decades, increasing temperature variability(IPCC, 2014) and changing monsoon behavior have raised concerns regarding future drought conditions and climate stress in northwestern Bangladesh(Jui et al., 2025). Previous studies mainly focused on rainfall variability, drought indices, or temperature trends separately(Rayhan & Rounak Afroz, 2024). However, integrated understanding of thermal dynamics, atmospheric moisture, and compound hydroclimatic conditions remains limited in the regional context.

Despite increasing hydroclimatic research worldwide, several important research gaps remain in Bangladesh. First, most previous studies analyzed climatic variables independently rather than examining the interaction among temperature, humidity, precipitation, and surface thermal conditions(Basak & Makin, 2025). Second, very limited studies investigated land–atmosphere coupling processes using Surface–Air Temperature Gradient (SATG), even though surface thermal dynamics strongly influence hydroclimatic behavior. Third, compound heat–dry events and hydroclimatic regime shifts have received very little attention in Bangladesh(Jingyi Hu et al., 2023), particularly at the regional scale. Existing drought studies also relied mainly on precipitation-based indicators and often ignored thermal feedback mechanisms. Unlike previous studies, this research develops an integrated hydroclimatic framework by combining SATG, Heat-Driven Dryness Index (HDDI), compound heat–dry event analysis, change-point detection, and spatial vulnerability assessment within a single regional assessment approach. In local environments such as Rajshahi Division, land–atmosphere coupling is highly important because dry soil conditions, intense surface heating, and reduced atmospheric moisture may alter regional hydroclimatic balance. Therefore, integrating surface and atmospheric thermal dynamics is necessary for understanding evolving climate stress and hydroclimatic transitions in northwestern Bangladesh.

Recent climate studies increasingly emphasize compound event analysis because climate hazards rarely occur independently(Zscheischler et al., 2018). Compound heat–dry events emerge when high thermal conditions interact with atmospheric moisture deficit and reduced precipitation. Such conditions can amplify environmental stress and influence agriculture, water resources, and ecosystem stability. To evaluate these interactions, this study integrates trend analysis, Surface–Air Temperature Gradient (SATG), Heat-Driven Dryness Index (HDDI), compound event detection, and change-point analysis within a unified hydroclimatic framework. Mann–Kendall trend analysis and Sen's slope estimator were applied to identify long-term changes in hydroclimatic variables(Kendall, 1975; Sen, 1968), while the Pettitt test was used to detect abrupt climate regime shifts(Pettitt, 1979). HDDI was developed by integrating standardized thermal and moisture variables to identify heat-driven dryness conditions. The frequency of compound heat–dry events was further evaluated to examine temporal variability and spatial vulnerability across districts. This methodological structure directly supports the research questions regarding hydroclimatic trends, land–atmosphere interactions, compound events, and regional climate transitions.

Northwestern Bangladesh is currently facing increasing hydroclimatic uncertainty due to changing temperature patterns, irregular rainfall distribution, and seasonal drought conditions. However, the long-term evolution of compound heat–dry interactions and hydroclimatic regime shifts remains insufficiently understood in Rajshahi Division. Therefore, this study aims to investigate long-term hydroclimatic changes and compound heat–dry dynamics in the region during 1992–2022. Specifically, the study seeks to: (1) quantify long-term trends and seasonal variability in surface temperature, air temperature, humidity, and precipitation; (2) detect hydroclimatic regime shifts and examine land–atmosphere thermal interactions using SATG; and (3) characterize the frequency, intensity, and spatial variability of compound heat–dry events using HDDI. The study is significant because it provides an integrated hydroclimatic assessment framework for northwestern Bangladesh by combining thermal dynamics, moisture variability, compound event analysis, and spatial vulnerability evaluation within a single analytical structure.

## 2. Study Area

The study was conducted in Rajshahi Division, located in northwestern Bangladesh between approximately 23.8°–25.2° N and 88.2°–89.8° E. The division comprises eight districts: Rajshahi, Chapai Nawabganj, Naogaon, Natore, Pabna, Sirajganj, Bogura, and Joypurhat (***Figure 1.***). The region experiences a tropical monsoon climate with strong seasonal variability in temperature and precipitation, where most rainfall occurs during the monsoon season(M. S. Islam et al., 2025).

Rajshahi Division is considered one of the hottest and most drought-prone regions of Bangladesh. Much of the area overlaps with the Barind Tract, an elevated Pleistocene terrace characterized by compact soils, low groundwater recharge, limited surface water availability, and low soil moisture retention capacity(Ferozur et al., 2019). These conditions increase the region's vulnerability to seasonal drought, thermal stress, and hydroclimatic variability.

The region is highly significant for hydroclimatic research because of its agricultural dependence, irregular rainfall distribution, and increasing groundwater stress. Frequent drought conditions and changing monsoon behavior make Rajshahi Division an important case study for investigating long-term hydroclimatic variability, land–atmosphere thermal interactions, and compound heat–dry events in northwestern Bangladesh.

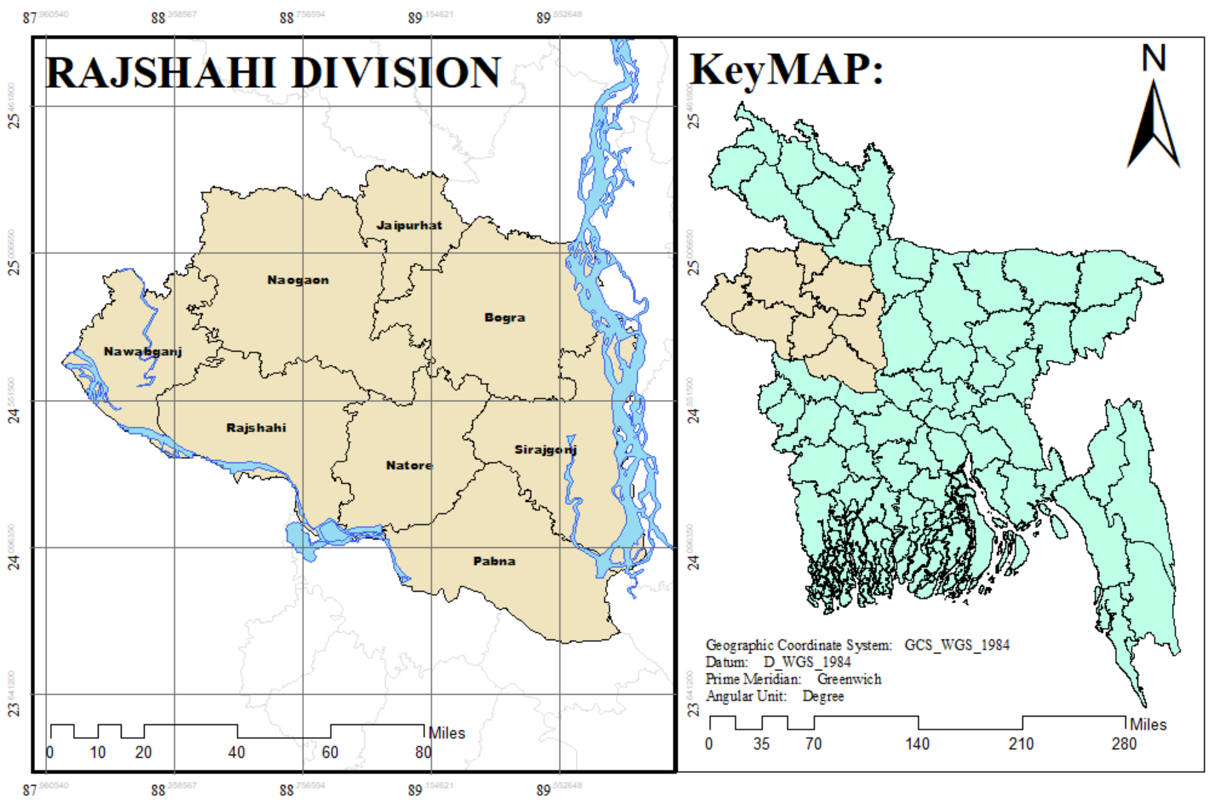


***Figure 1. Location of Rajshahi Division in Bangladesh and administrative boundaries of the eight districts analyzed in this study.***

## *3. Methodology*

### 3.1 Data Sources and Hydroclimatic Variables

Monthly hydroclimatic data from January 1992 to December 2022 were obtained from the National Aeronautics and Space Administration open-access NASA Prediction Of Worldwide Energy Resources (POWER) database(NASA, 2020). The NASA POWER dataset integrates satellite observations, reanalysis outputs, and assimilated ground measurements to provide spatially consistent climate information widely used in environmental and climate research.

Data were extracted for the eight districts of Rajshahi Division using district centroid coordinates. Four key variables representing regional land–atmosphere hydroclimatic conditions were selected: Earth Skin Temperature (°C), Air Temperature at 2 m (°C), Specific Humidity at 2 m (g $kg^{-1}$), and Precipitation Corrected Sum (mm). These variables collectively describe thermal conditions, atmospheric moisture, and precipitation variability.

Monthly temporal resolution was used to evaluate seasonal variability and long-term hydroclimatic trends. District-level datasets were compiled into continuous time series, while division-wide averages were calculated for regional analysis. Although the Bangladesh Meteorological Department provides ground observations, long-term and spatially continuous records for all selected variables were not consistently available across the study area. Therefore, NASA POWER data were used to ensure standardized and continuous observations throughout the study period.

### 3.2 Data Pre-Processing and Temporal Aggregation

Prior to statistical analysis, all hydroclimatic datasets underwent a structured pre-processing procedure to ensure temporal consistency, data reliability, and inter-district comparability across Rajshahi Division. Monthly observations were organized into continuous time series using year and month identifiers. Data quality assessment included visual screening for anomalous values, verification of unit consistency, and detection of incomplete records. Minor missing observations were corrected using temporal interpolation to preserve data continuity while minimizing distortion of long-term climatic signals.

To investigate hydroclimatic variability at multiple temporal scales, monthly observations were aggregated into seasonal and annual series following the (***Table 1.***) climatological convention commonly used in Bangladesh. This seasonal framework enabled assessment of monsoon-driven variability, pre-monsoon thermal stress, and winter dryness characteristics across the study region.

***Table 1. Seasonal classification used in the study.***

| **Season** | **Months** |
|---|---|
| **Winter** | December – February |
| **Pre-monsoon** | March – May |
| **Monsoon** | June – September |
| **Post-monsoon** | October – November |

District-level datasets were retained to preserve spatial heterogeneity among the eight districts, while division-wide mean series were generated to evaluate broader regional hydroclimatic behavior. Prior to composite index development and integrated multi-variable analysis, selected variables were standardized using z-score normalization to reduce scale dependency and improve comparability among thermal, moisture, and precipitation variables.

### *3.3 Trend Analysis & Evaluation*

Long-term hydroclimatic trends were evaluated using the Mann–Kendall Test(Kendall, 1975), a non-parametric statistical method widely applied in climatological and hydrological studies due to its robustness against non-normal data distributions and missing values. The test identifies the presence of monotonic trends in time-series data.

For a time series $x_1, x_2, \ldots, x_n$, the Mann–Kendall statistic $S$is calculated as:

$$S = \sum_{i=1}^{n-1} \sum_{j=i+1}^{n} \operatorname{sgn}(x_j - x_i) \tag{1}$$

Where,

$$\operatorname{sgn}(x_j - x_i) = \begin{cases} 1 & x_j - x_i > 0 \\ 0 & x_j - x_i = 0 \\ -1 & x_j - x_i < 0 \end{cases}$$

The significance of the trend was assessed using the standardized test statistic $Z$.

To quantify the magnitude of detected trends, Sen's Slope Estimator(Sen, 1968) was applied. Sen's slope estimates the median rate of change between all possible data pairs:

$$Q = \text{median}\left(\frac{x_j - x_i}{j - i}\right), j > i \tag{2}$$

Trend analysis was conducted for annual and seasonal time series of air temperature, earth skin temperature, specific humidity, precipitation, SATG, and HDDI and evaluation insight following by (***Table. 2***)

*Table 2. Interpretation of Mann–Kendall trend results*

| MK Output | Interpretation |
|---|---|
| **Trend = Increasing** | Variable shows upward trend |
| **Trend = Decreasing** | Variable shows downward trend |
| **h = True** | Trend statistically significant |
| **h = False** | Trend not significant |
| **p < 0.05** | Significant at 95% confidence |

### 3.4 Change-Point Detection (Regime Shift Analysis)

To identify abrupt shifts in hydroclimatic regimes, change-point analysis was conducted using the Pettitt Test(Pettitt, 1979), a widely used non-parametric method for detecting structural breaks in time-series data.

The Pettitt statistic $U_t$is computed as:

$$U_t = \sum_{i=1}^{t} \sum_{j=t+1}^{n} \mathrm{sgn}( x_j - x_i) \tag{3}$$

where $x_i$and $x_j$represent observations at different time steps.

The year corresponding to the maximum absolute value of $U_t$represents the most probable change point in the series. Statistical significance was evaluated using the associated p-value, with $p < 0.05$ indicating a significant regime shift. Change-point analysis was applied to annual hydroclimatic variables and compound event frequency to detect potential shifts in the regional hydroclimatic regime.

### 3.5 Land–Atmosphere Thermal Gradient Analysis

To assess land–atmosphere thermal coupling, the Surface–Air Temperature Gradient (SATG) was calculated as the difference between land surface temperature and near-surface air temperature(Good, 2016).

$$SATG = T_{skin} - T_{air} \tag{4}$$

Where, $T_{skin}$= Earth skin temperature (°C), $T_{air}$= air temperature at 2 m (°C)

Positive SATG values indicate stronger surface heating relative to the atmosphere, while negative values suggest reduced surface–atmosphere thermal contrast. SATG provides an indicator of surface energy imbalance and potential heat-driven drying processes(Dey et al., 2025). Seasonal and annual SATG series were analyzed using the same trend detection approach described above.

### 3.5 Development of the Heat-Driven Dryness Index (HDDI)

To quantify compound hydroclimatic stress, a Heat-Driven Dryness Index (HDDI) was developed by integrating standardized thermal and moisture variables. The index was designed to capture the combined influence of atmospheric heating and moisture deficiency within a single hydroclimatic framework. Unlike conventional drought indicators that rely primarily on precipitation variability, HDDI incorporates both surface thermal dynamics and atmospheric moisture conditions to better represent compound heat–dry interactions.

Prior to index calculation, all variables were normalized using z-score standardization(Duran, 2017) to remove scale differences and ensure inter-variable comparability:

$$Z = \frac{X - \mu}{\sigma} \qquad (5)$$

Where, $X$= observed value, $\mu$= mean, $\sigma$= standard deviation.

Following composite hydroclimatic index approaches, HDDI was formulated by integrating temperature-related and moisture-related anomalies:

$$HDDI = \frac{Z(T_{air}) + Z(T_{skin}) - Z(Humidity) - Z(Precipitation)}{4} \qquad (6)$$

The inclusion of both air temperature and earth skin temperature allows the index to represent land–atmosphere thermal coupling, while humidity and precipitation components capture atmospheric and hydrological moisture availability. This integrated structure provides a more comprehensive representation of hydroclimatic stress under monsoon-influenced environmental conditions.

Following (***Table 3.***) positive HDDI values indicate conditions characterized by higher temperatures and reduced moisture availability, representing heat-driven dryness, whereas negative values indicate relatively humid or less thermally stressed conditions. Seasonal and annual HDDI time series were subsequently analyzed using the Mann–Kendall test and Sen's slope estimator to detect long-term hydroclimatic trends(Shaha & Kiran, 2021).

***Table 3. Applications of HDDI values in finding***

| **HDDI value** | **Interpretation** |
|---|---|
| **HDDI > 0** | Heat-driven dryness conditions |
| **HDDI ≈ 0** | Neutral hydroclimatic state |
| **HDDI < 0** | Moist or humid conditions |

### 3.6 Identification of Compound Heat–Dry Events

Compound hydroclimatic extremes occur when multiple climate stressors interact simultaneously. In this study, compound heat–dry events were identified using the Heat-Driven Dryness Index (HDDI), which integrates standardized temperature and moisture variables.

Monthly HDDI values were computed for each district and subsequently aggregated into annual series. A compound heat–dry event was defined as a month when:

$$HDDI > 0$$

This threshold indicates simultaneous thermal intensification and moisture deficit conditions relative to the climatological mean. The annual frequency of compound events was calculated as the number of months within each year satisfying the above condition.

The resulting time series of annual compound event counts was used to evaluate temporal variability according to (***Table 4.***) and long-term trends in hydroclimatic stress across Rajshahi Division.

***Table 4. Definition of compound heat–dry events.***

| Condition | Interpretation |
|---|---|
| **HDDI > 0** | Heat-driven dry conditions |
| **HDDI ≤ 0** | Non-compound conditions |

### 3.7 Spatial Vulnerability Assessment

To evaluate spatial differences in hydroclimatic stress across Rajshahi Division, a district-level vulnerability index was developed by integrating two key indicators:

1. Long-term HDDI trends
2. Frequency of compound heat–dry events

Prior to integration, both variables were normalized using min–max scaling(Kim et al., 2025):

$$X_{norm} = \frac{X - X_{min}}{X_{max} - X_{min}} \quad (7)$$

The vulnerability index for each district was then calculated as:

$$VI = \frac{HDDI_{norm} + Events_{norm}}{2} \quad (8)$$

Where, $HDDI_{norm}$= normalized HDDI trend magnitude, $Events_{norm}$= normalized compound event frequency

Higher index values indicate greater vulnerability to heat-driven dryness, while lower values represent relatively stable hydroclimatic conditions(IPCC, 2014). The resulting index (***Table 5.***)

was used to compare spatial patterns of hydroclimatic vulnerability among the eight districts of Rajshahi Division.

***Table 5. Vulnerability index allign with the HDDI and Components events.***

| **Vulnerability Index** | **Interpretation** |
|---|---|
| VI > 0.75 | High vulnerability |
| 0.50 – 0.75 | Moderate vulnerability |
| 0.25 – 0.50 | Low vulnerability |
| < 0.25 | Very low vulnerability |

### *3.8 Analytical Workflow*

To ensure a systematic analytical framework, the study followed a multi-step workflow integrating data preprocessing, statistical analysis, and spatial assessment (***Figure 2.***).

The workflow begins with extraction of monthly hydroclimatic data from the NASA POWER database for the eight districts of Rajshahi Division. After quality control and seasonal aggregation, long-term trends were evaluated using the Mann–Kendall test and Sen's slope estimator. Surface–Air Temperature Gradient (SATG) and the Heat-Driven Dryness Index (HDDI) were subsequently calculated to assess land–atmosphere thermal interactions and compound hydroclimatic stress.

The HDDI series was then used to identify compound heat–dry events and compute annual event frequencies. Change-point analysis using the Pettitt test was applied to detect abrupt shifts in hydroclimatic conditions. Finally, district-level vulnerability was assessed by combining HDDI trends and compound event frequency into a composite vulnerability index.

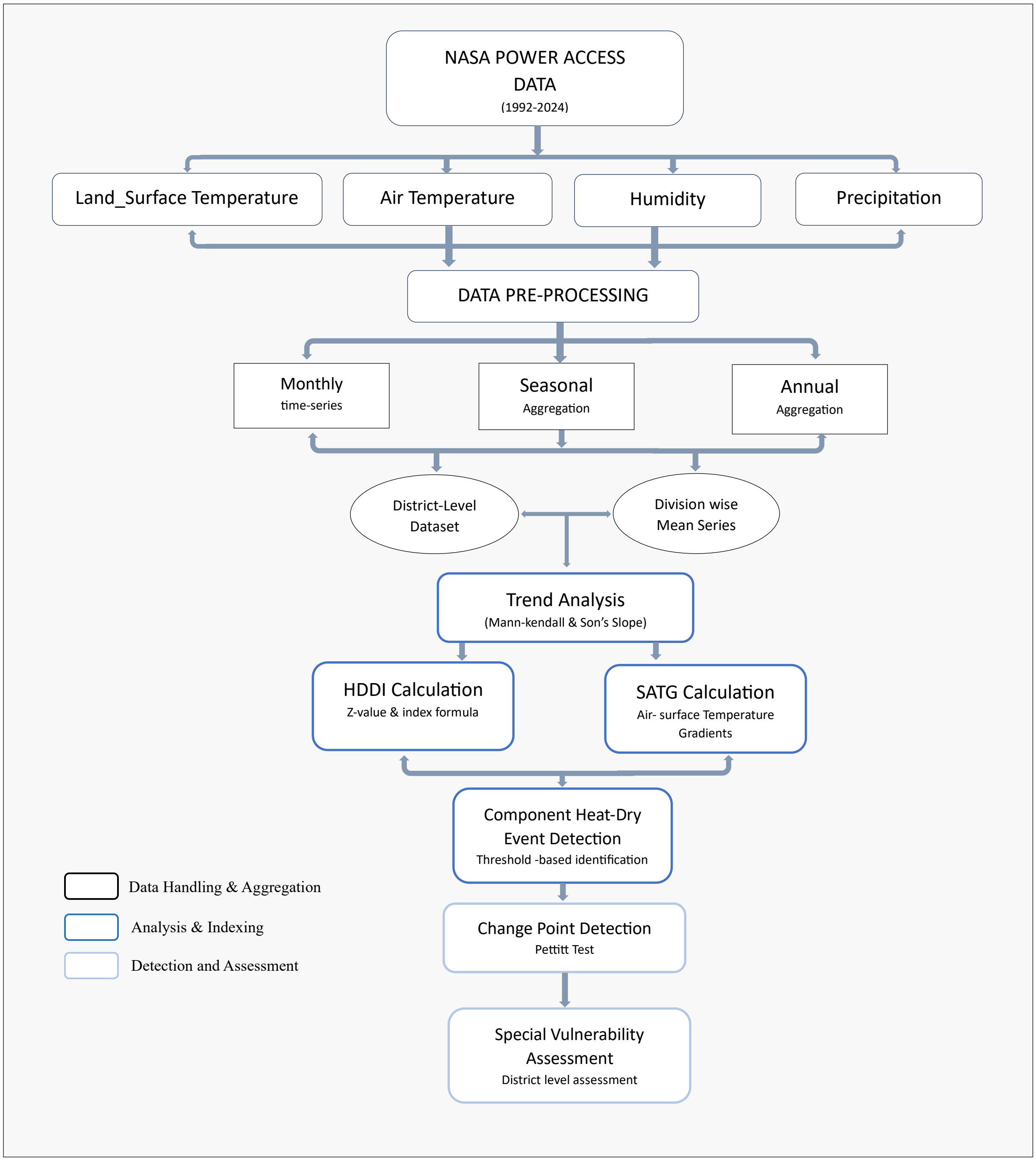


*Figure. 2. Methodological workflow.*

# 4.Result

## 4.1 Assess long-term trends and seasonal variability

### 4.1.1 Temporal Variability of Hydroclimatic Variables (1992–2022)

The annual hydroclimatic time series of Rajshahi Division from 1992 to 2022 demonstrated considerable interannual variability in both thermal and moisture-related variables (***Figure 3 a–d***). Annual mean air temperature ranged from approximately 24.8°C to 27.5°C, with comparatively higher values observed during the early 1990s, particularly between 1992 and 1996 when temperatures frequently exceeded 27°C. Earth skin temperature showed a similar temporal pattern, varying between about 24.7°C and 28.3°C, with peak values recorded during the early study period and relatively lower fluctuations after the late 1990s.

Specific humidity varied from nearly 11.4 to 15.7 g kg$^{-1}$. Lower humidity conditions were evident during the early 1990s, while values generally remained above 14 g kg$^{-1}$ after the late 1990s. Precipitation exhibited the highest temporal variability among all variables, ranging from approximately 30 mm to more than 210 mm annually. Several high-rainfall years were observed after 2015, whereas comparatively lower precipitation conditions occurred during the early 1990s. Overall, the hydroclimatic variables displayed distinct temporal fluctuations and seasonal irregularities throughout the study period.

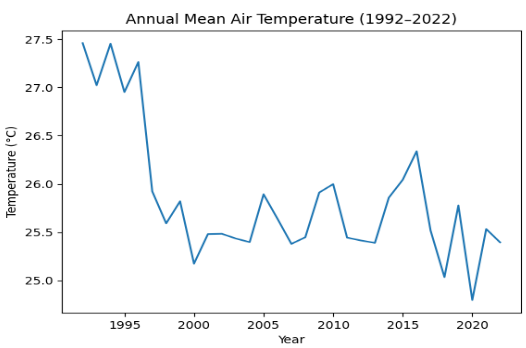


(3.a) Air temperature

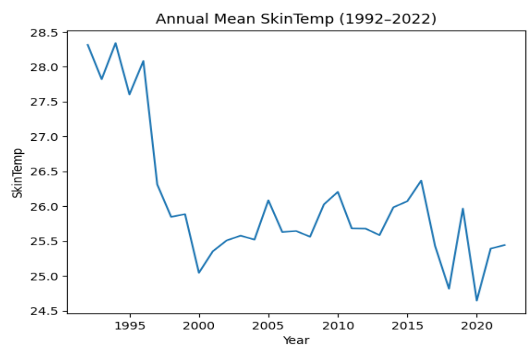


(3.b) Earth skin temperature

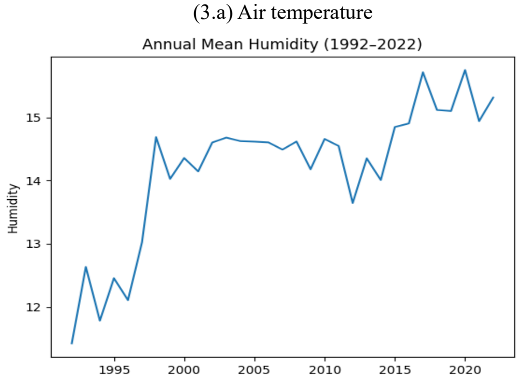


(3.c) Specific humidity

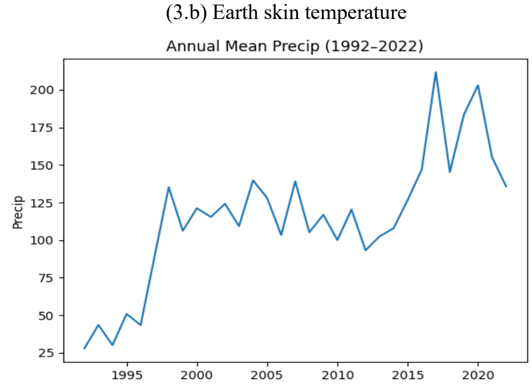


(3.d) Precipitation

***Figure (3 a-d). Annual mean time series of air temperature, Earth skin temperature, specific humidity, and precipitation in Rajshahi Division (1992–2022).***

### 4.1.2 Long-Term Trends in Hydroclimatic Variables

Trend analysis using linear regression, the Mann–Kendall (MK) test (***Eq.1***), and Sen's slope(***Eq.2***) estimator revealed statistically significant long-term changes in the hydroclimatic conditions of Rajshahi Division during 1992–2022 (***Table 6.***). Air temperature exhibited a significant decreasing trend (MK $Z = -2.72$, $p = 0.0065$), with a linear decline rate of −0.046 °C $yr^{-1}$ and a Sen's slope of −0.0316 °C $yr^{-1}$. Earth skin temperature showed a comparatively stronger negative trend (MK $Z = -2.65$, $p = 0.0080$), declining at approximately −0.069 °C $yr^{-1}$ with a Sen's slope of −0.0451 °C $yr^{-1}$.

In contrast, moisture-related variables displayed increasing trends throughout the study period. Specific humidity recorded a highly significant positive trend (MK $Z = +4.62$, $p < 0.001$), with a linear increase of +0.0949 g $kg^{-1}$ $yr^{-1}$ and a Sen's slope of +0.0756 g $kg^{-1}$ $yr^{-1}$. Precipitation also increased significantly (MK $Z = +4.08$, $p < 0.001$), exhibiting the highest rate of change among all variables, with a linear slope of +3.717 mm $yr^{-1}$ and a Sen's slope of +3.636 mm $yr^{-1}$. Kendall's Tau values further confirmed strong negative associations for thermal variables and positive associations for humidity and precipitation.

***Table 6. Long-term trends of hydroclimatic variables in Rajshahi Division (1992–2022).***

| Variable | Linear Slope | Sen's Slope | MK Z | p-value | Kendall's Tau | Trend Interpretation |
|---|---|---|---|---|---|---|
| **Air Temperature (2 m)** | −0.0464 °C/yr | -0.0316 | -2.72 | 0.00654 | -0.346 | Significant decrease |
| **Earth Skin Temperature** | −0.0695 °C/yr | -0.0451 | -2.65 | 0.00801 | -0.338 | Significant decrease |
| **Specific Humidity** | +0.0949 g/kg/yr | +0.0756 | +4.62 | $3.78\times10^{-6}$ | +0.587 | Highly significant increase |
| **Precipitation** | +3.717 mm/yr | +3.636 | +4.08 | $4.52\times10^{-5}$ | +0.518 | Highly significant increase |

### 4.1.3 Seasonal Variations and Trends

Seasonal hydroclimatic variability in Rajshahi Division showed distinct fluctuations across thermal and moisture-related variables during 1992–2022 (***Figures 4 a-p.***). Pre-monsoon air temperature remained comparatively high, generally fluctuating between 28°C and 32°C, while monsoon temperatures mostly ranged from 28.4°C to 31.3°C. Post-monsoon temperatures varied between approximately 21.5°C and 26.3°C, whereas winter temperatures remained comparatively lower, ranging from nearly 17.3°C to 20.6°C. Earth skin temperature exhibited similar seasonal behavior but with slightly higher magnitudes, reaching above 33°C during the pre-monsoon season and declining to nearly 16.5°C during winter.

Specific humidity displayed strong seasonal contrasts, with monsoon values exceeding 20 g $kg^{-1}$ in most years, while winter humidity generally fluctuated between 5 and 9 g $kg^{-1}$. Precipitation variability was highest during the monsoon season, where rainfall frequently exceeded 250 mm and reached over 400 mm in several years. In contrast, winter precipitation mostly remained below 20 mm, while post-monsoon rainfall exhibited highly irregular interannual fluctuations.

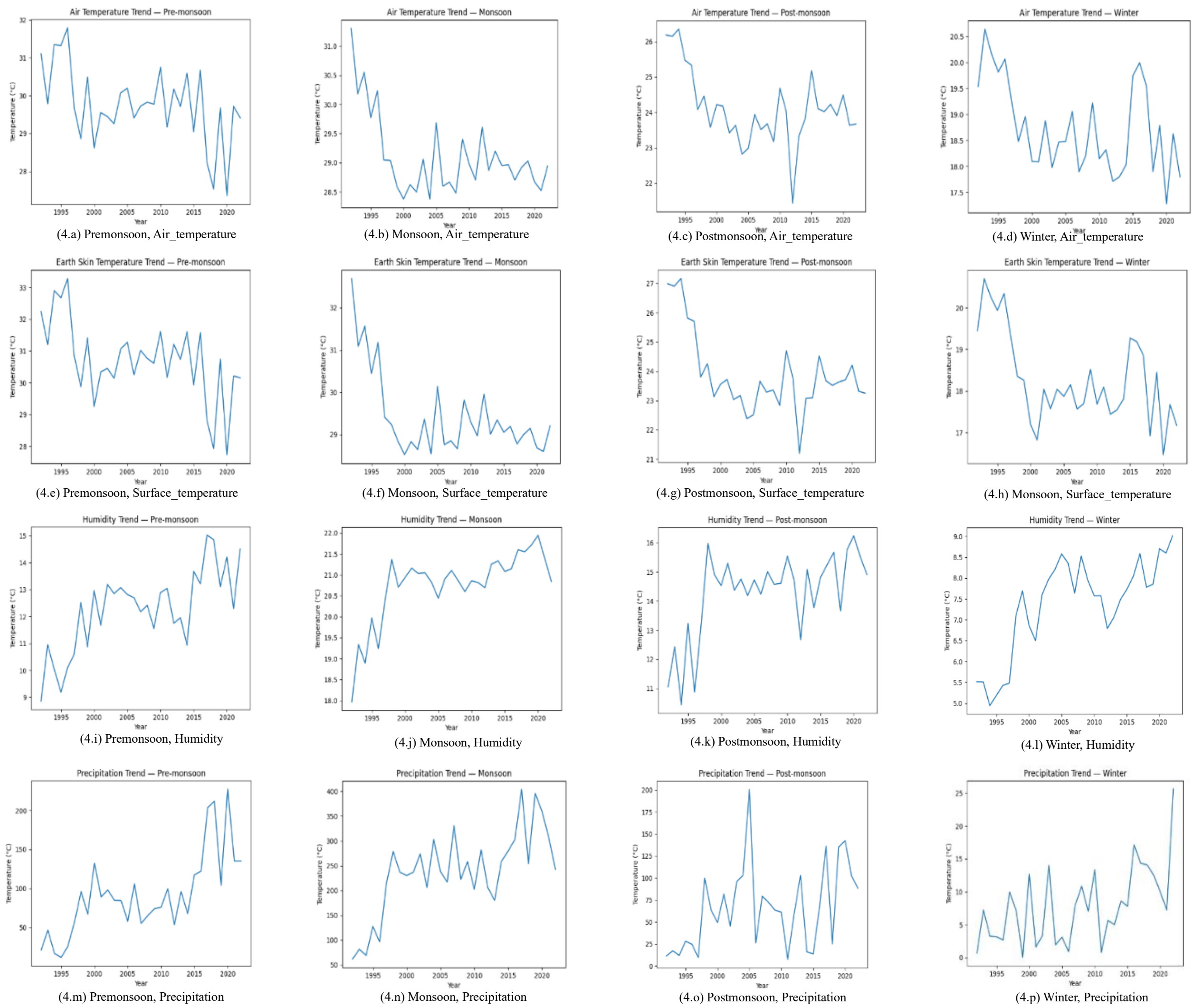


(4.a) Premonsoon, Air_temperature (4.b) Monsoon, Air_temperature (4.c) Postmonsoon, Air_temperature (4.d) Winter, Air_temperature

(4.e) Premonsoon, Surface_temperature (4.f) Monsoon, Surface_temperature (4.g) Postmonsoon, Surface_temperature (4.h) Monsoon, Surface_temperature

(4.i) Premonsoon, Humidity (4.j) Monsoon, Humidity (4.k) Postmonsoon, Humidity (4.l) Winter, Humidity

(4.m) Premonsoon, Precipitation (4.n) Monsoon, Precipitation (4.o) Postmonsoon, Precipitation (4.p) Winter, Precipitation

***Figure 4 a-p. Evolution of Seasonal Heat-Driven Dryness with hydro-variables of Rajshahi Division.***

## 4.4 Seasonal Trend Characteristics of Hydroclimatic Variables

Seasonal trend analysis revealed notable temporal variations among thermal and moisture-related variables across Rajshahi Division during 1992–2022 (***Table 7.***). Using (***Eq.1 & Eq.2***) Air temperature exhibited negative linear trends in all seasons, ranging from approximately −0.038 °C yr$^{-1}$ during the monsoon season to −0.054 °C yr$^{-1}$ during the pre-monsoon period. Winter air temperature also showed a marked decline of nearly −0.045 °C yr$^{-1}$. Earth skin temperature displayed stronger negative trends than air temperature throughout all seasons, with the largest decline occurring during the post-monsoon season (−0.079 °C yr$^{-1}$), followed by pre-monsoon conditions (−0.076 °C yr$^{-1}$). Monsoon and winter earth skin temperatures also declined by more than −0.06 °C yr$^{-1}$, indicating persistent seasonal surface cooling patterns across the study region. Seasonal thermal variability was particularly pronounced during the late 1990s and early 2000s, when several abrupt fluctuations were observed across both atmospheric and surface temperature records.

In contrast, specific humidity increased consistently across all seasons. The strongest increase was observed during the pre-monsoon season (+0.124 g $kg^{-1}$ $yr^{-1}$), while monsoon humidity increased by approximately +0.069 g $kg^{-1}$ $yr^{-1}$. Precipitation also exhibited positive seasonal trends, particularly during the monsoon season where rainfall increased by nearly +6.71 mm $yr^{-1}$. Comparatively smaller increases were observed during winter (+0.363 mm $yr^{-1}$) and post-monsoon periods (+2.08 mm $yr^{-1}$).

**Table 7.** Seasonal trend statistics of hydroclimatic variables (Sen's slope and Mann–Kendall results).

| Variable | Season | Linear Slope | Sen's Slope | MK Z | p-value | Tau |
|---|---|---|---|---|---|---|
| **Air Temperature** | Pre-monsoon | −0.054 | −0.041 | −2.18 | 0.0296 | −0.277 |
| | Monsoon | −0.038 | −0.026 | −1.84 | 0.0664 | −0.234 |
| | Post-monsoon | −0.052 | −0.044 | −1.94 | 0.0527 | −0.247 |
| | Winter | −0.045 | −0.049 | −2.89 | 0.00386 | −0.368 |
| **Earth Skin Temperature** | Pre-monsoon | −0.076 | −0.066 | −2.58 | 0.00978 | −0.329 |
| | Monsoon | −0.063 | −0.042 | −2.24 | 0.0249 | −0.286 |
| | Post-monsoon | −0.079 | −0.050 | −2.04 | 0.0414 | −0.260 |
| | Winter | −0.066 | −0.063 | −2.92 | 0.00346 | −0.372 |
| **Specific Humidity** | Pre-monsoon | +0.124 | +0.123 | +3.98 | $6.97\times10^{-5}$ | +0.505 |
| | Monsoon | +0.069 | +0.055 | +4.15 | $3.37\times10^{-5}$ | +0.527 |
| | Post-monsoon | +0.098 | +0.085 | +3.30 | 0.00098 | +0.419 |
| | Winter | +0.097 | +0.101 | +4.22 | $2.50\times10^{-5}$ | +0.535 |
| **Precipitation** | Pre-monsoon | +4.172 | +3.634 | +4.28 | $1.84\times10^{-5}$ | +0.544 |
| | Monsoon | +6.709 | +6.485 | +3.77 | 0.000161 | +0.480 |
| | Post-monsoon | +2.082 | +2.443 | +2.28 | 0.0228 | +0.290 |
| | Winter | +0.363 | +0.330 | +2.89 | 0.00386 | +0.368 |

## 4.2 Surface–Air Temperature Gradient (SATG)

### *4.2.1 Annual Surface–Air Temperature Gradient (SATG)*

The annual Surface–Air Temperature Gradient (SATG) in Rajshahi Division exhibited substantial temporal variability during 1992–2022 (***Figure 5.***). SATG values from ***Eq.4*** remained strongly positive during the early 1990s, fluctuating between approximately 0.65°C and 0.88°C. A rapid decline occurred after the mid-1990s, with SATG decreasing to nearly −0.13°C around 1999–2000. Between 2001 and 2014, the gradient generally fluctuated within a comparatively narrow range of about 0.00°C to 0.27°C. Negative SATG values reappeared after 2016, reaching nearly −0.22°C around 2018 before partially recovering toward 0.05°C by 2022. Interannual fluctuations were particularly evident during the late 1990s and late 2010s, indicating substantial variability in the thermal difference between surface and near-surface atmospheric conditions throughout the study period.

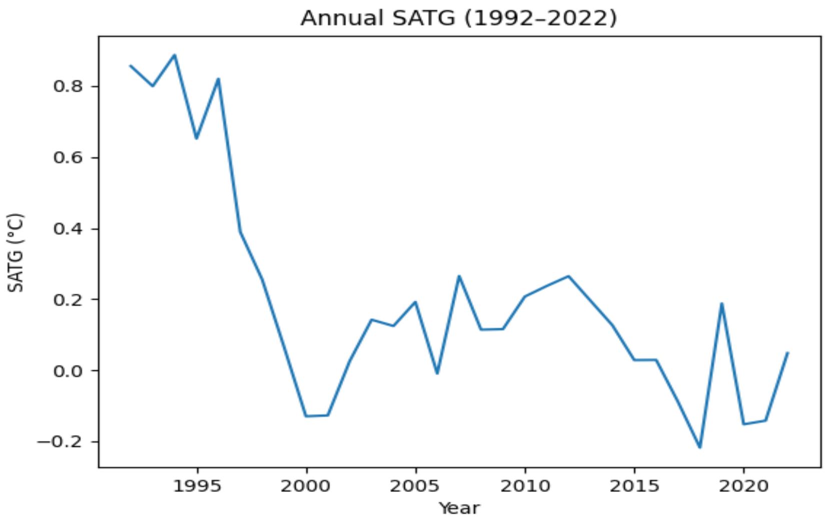


***Figure 5. Annual Surface–Air Temperature Gradient (SATG)***

#### *4.2.2 Seasonal Surface–Air Temperature Gradient (SATG)*

Seasonal SATG patterns demonstrated considerable variability across climatic seasons in Rajshahi Division during 1992–2022 (***Figures 6 a–d.***). Pre-monsoon SATG recorded the highest values among all seasons, ranging from approximately 0.38°C to 1.55°C. Comparatively elevated gradients were observed during the early 1990s, while lower values occurred after 2017. Monsoon SATG fluctuated between nearly 0.01°C and 1.38°C, with a pronounced decline after the mid-1990s and relatively stable lower values after 2000.

Post-monsoon SATG displayed both positive and negative conditions, varying from approximately −0.73°C to 0.82°C. Negative gradients became more frequent after the late 1990s, particularly during the mid-2010s. Winter SATG exhibited the lowest values overall, ranging from nearly −1.27°C to 0.28°C. Strong negative winter gradients were observed around 2000 and again after 2016, while comparatively weak positive conditions occurred during the early 1990s. Seasonal fluctuations remained evident throughout the entire observation period across all four climatic seasons.

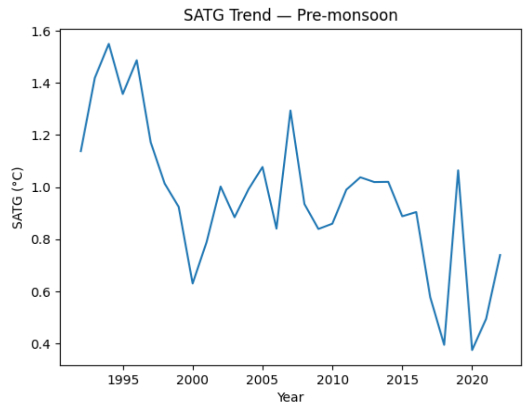


(6.a) Premonsoon, SATG

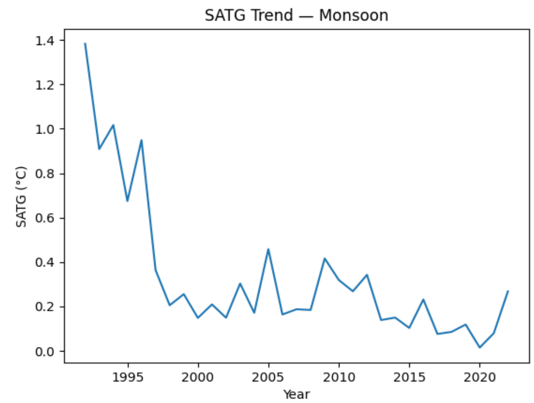


(6.b) Monsoon, SATG

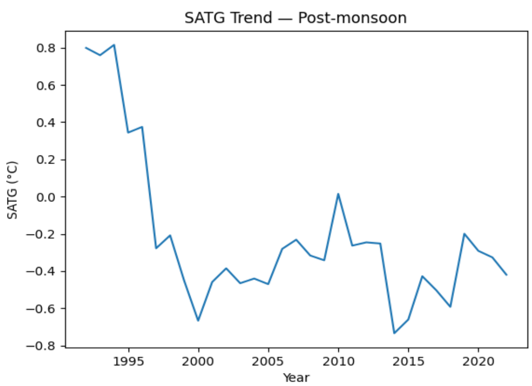


(6.c) Postmonsoon, SATG

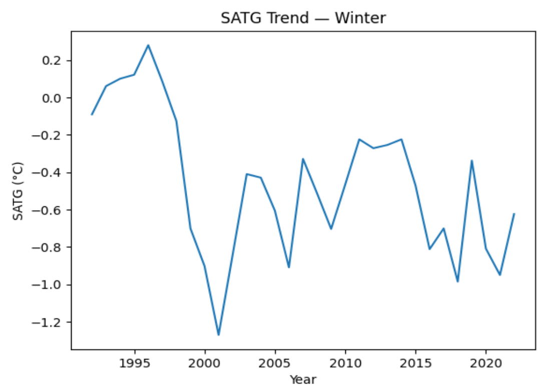


(6.d) Winter, STAG

***Figure 6 a-d. Evolution of Seasonal Surface–Air Temperature Gradient of Rajshahi Division.***

### 4.2.3 Seasonal Trends of Surface–Air Temperature Gradient (SATG).

Seasonal trend statistics revealed consistent negative trends in Surface–Air Temperature Gradient (SATG) across all climatic seasons in Rajshahi Division during 1992–2022 (***Table 8.***). The strongest linear decline was observed during the post-monsoon season (−0.0270 °C $yr^{-1}$), followed closely by the monsoon season (−0.0244 °C $yr^{-1}$). Pre-monsoon SATG also decreased substantially at approximately −0.0214 °C $yr^{-1}$, while winter exhibited a comparatively lower decline rate of −0.0206 °C $yr^{-1}$.

Mann–Kendall statistics indicated statistically significant decreasing trends for all seasons. The monsoon season recorded the strongest negative association (MK Z = −4.08; Tau = −0.518), followed by the pre-monsoon period (MK Z = −3.37; Tau = −0.428). Winter and post-monsoon seasons also showed significant negative trends, with MK Z values of −2.50 and −2.21, respectively. Sen's slope estimates further confirmed declining SATG conditions throughout the study period, with values ranging from approximately −0.0150 °C $yr^{-1}$ during post-monsoon to −0.0209 °C $yr^{-1}$ during winter and pre-monsoon periods.

***Table 8. Seasonal trends of Surface–Air Temperature Gradient (SATG), 1992–2022***

| Season | Linear Slope (°C/yr) | Sen's Slope (°C/yr) | MK Z | p-value | Kendall's Tau |
|---|---|---|---|---|---|
| **Winter** | -0.0206 | -0.0209 | -2.50 | 0.0125 | -0.318 |
| **Pre-monsoon** | -0.0214 | -0.0209 | -3.37 | 0.00076 | -0.428 |
| **Monsoon** | -0.0244 | -0.0145 | -4.08 | $4.52\times10^{-5}$ | -0.518 |
| **Post-monsoon** | -0.0270 | -0.0150 | -2.21 | 0.0271 | -0.282 |

## 4.3 Heat-Driven Dryness Index (HDDI)

### 4.3.1 Seasonal Evolution of Heat-Driven Dryness (1992–2022)

Seasonal HDDI variability in Rajshahi Division showed substantial fluctuations between 1992 and 2022 (***Figures 7 a–d***). The pre-monsoon season recorded by ***Eq.6*** the highest HDDI values among all seasons, ranging from approximately −0.5 to above 4.4. Extremely high values were observed during the early 1990s, while comparatively lower and more variable conditions appeared after 2015. Several years after 2017 approached neutral or slightly negative conditions.

Monsoon HDDI fluctuated between nearly −3.2 and 2.2. Positive values dominated during the early 1990s, whereas negative values became more frequent after the late 1990s. Strong negative conditions were particularly visible after 2015, when HDDI frequently remained below −2.0.

Post-monsoon HDDI ranged from approximately −2.4 to 2.0 and exhibited strong interannual variability throughout the study period. Negative conditions became increasingly common after the late 1990s, although several short-term positive fluctuations occurred during the mid-2010s.

Winter HDDI displayed comparatively lower variability, fluctuating between about −1.7 and 0.5. Early winter conditions remained slightly positive, while negative values dominated after the late 1990s and persisted throughout most recent years.

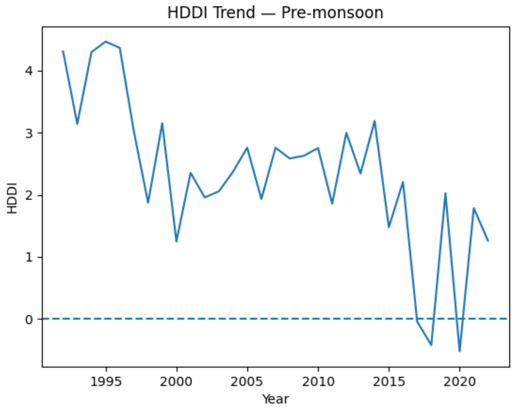


(7.a) Premonsoon, HDDI

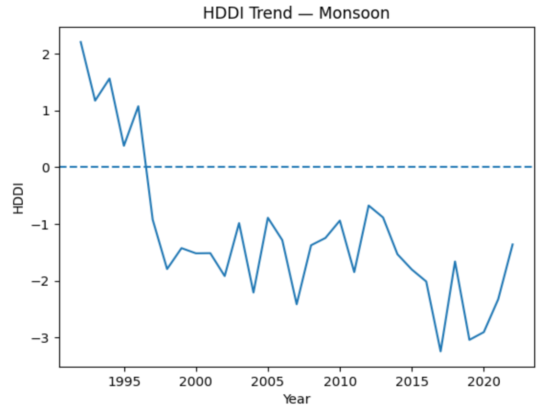


(7.b) Monsoon, HDDI

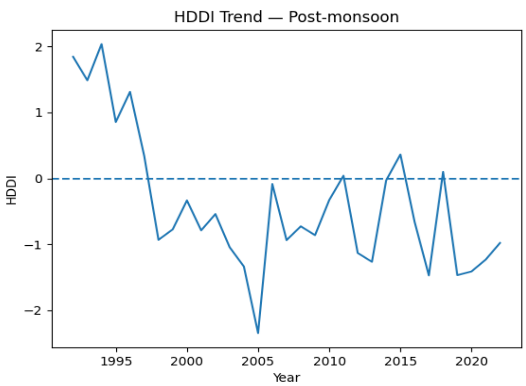


(7.c) Postmonsoon, HDDI

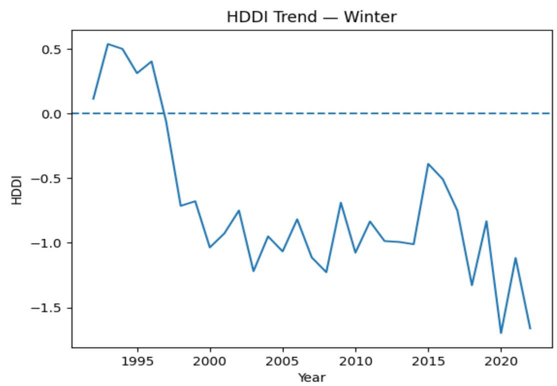


(7.d) Winter, HDDI

***Figure 7. Evolution of Seasonal Heat-Driven Dryness of Rajshahi Division.***

### 4.3.2 Seasonal Trends of Heat-Driven Dryness Index (HDDI)

Seasonal trend statistics revealed persistent declines in HDDI across all climatic seasons in Rajshahi Division during 1992–2022 (***Table 9.***). The strongest decrease was observed during the monsoon season, where the linear decline rate reached approximately −0.101 $yr^{-1}$ with a Sen's slope of −0.0897 $yr^{-1}$ from ***Eq.4***. Pre-monsoon HDDI also showed a pronounced decline, with a linear slope of nearly −0.093 $yr^{-1}$ and a Sen's slope of −0.0821 $yr^{-1}$. Winter HDDI decreased at a comparatively lower rate of approximately −0.046 $yr^{-1}$.

Mann–Kendall statistics further indicated strong negative associations for all seasons. Winter recorded the strongest negative Kendall's Tau value (−0.475), followed by pre-monsoon (−0.467) and monsoon (−0.449) conditions. MK Z values ranged between −3.54 and −3.74, while p-values remained below 0.001 for all seasons, indicating strong statistical significance. The seasonal decline rates and negative association values collectively demonstrate substantial temporal variability in heat-driven dryness conditions throughout the study period.

**Table 9. Seasonal trends of Heat-Driven Dryness Index (HDDI), 1992–2022.**

| Season | Linear Slope (per year) | Sen's Slope | MK Z | p-value | Kendall's Tau |
|---|---|---|---|---|---|
| **Winter** | -0.0460 | -0.0424 | -3.74 | 0.00018 | -0.475 |
| **Pre-monsoon** | -0.0929 | -0.0821 | -3.67 | 0.00024 | -0.467 |
| **Monsoon** | -0.1009 | -0.0897 | -3.54 | 0.00041 | -0.449 |
| **Post-monsoon** | -0.0673 | -0.0570 | -2.96 | 0.00041 | -0.376 |

## 4.4 Compound Heat–Dry Events

### 4.4.1 Temporal Evolution of Compound Heat–Dry Events (1992–2022)

The annual frequency of compound heat–dry events in Rajshahi Division showed considerable interannual variability during 1992–2022 (Figure 8.). The highest event frequency occurred during the early 1990s, when annual occurrences frequently exceeded 25 events and reached nearly 30 events in 1992. Comparatively high frequencies were also observed around 1994 and 1996, with annual counts remaining above 20 events.

After the late 1990s, event frequency became relatively lower and more irregular. During the 2000s and early 2010s, annual occurrences generally fluctuated between 8 and 16 events. Several moderate increases were observed around 2004, 2008, and 2013, when frequencies temporarily rose above 15 events. In contrast, substantially lower event frequencies appeared after 2015, particularly around 2017 and 2020, when annual occurrences declined to below 5 events. The final years of the study period showed partial recovery, with event frequency increasing again to approximately 13–16 events by 2021–2022.

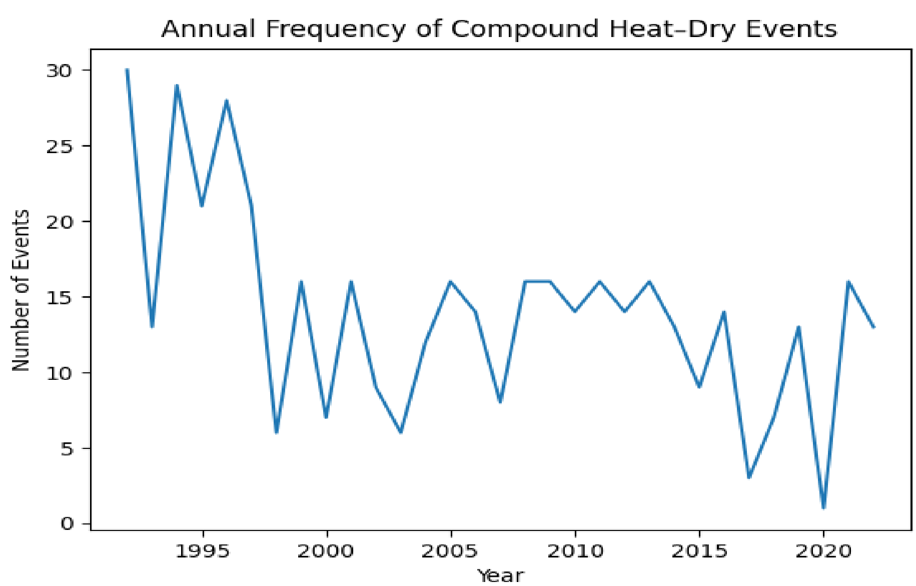


**Figure 8.** Annual frequency of compound heat–dry events in Rajshahi Division (1992–2022).

### 4.4.2 Trend Analysis of Event Frequency and Overall Magnitude

Trend statistics indicated a long-term decline in the frequency of compound heat–dry events across Rajshahi Division during 1992–2022 (***Table 10.***). Linear regression analysis showed a negative slope of approximately −0.384 events $yr^{-1}$, while Sen's slope estimated a median decline rate of nearly −0.300 events $yr^{-1}$. Mann–Kendall analysis also indicated a statistically significant negative trend, with an MK Z value of −2.44 and Kendall's Tau of −0.308.

The frequency of compound heat–dry events accounted for approximately 14.55% of total monthly observations during the study period. The negative slope values and declining association statistics correspond closely with the temporal evolution shown in Figure 4.7, where higher event frequencies during the early 1990s gradually transitioned toward comparatively lower and less persistent occurrences after the late 1990s. Statistical significance was confirmed by a p-value of 0.0145, indicating that the declining event frequency was unlikely to result from random temporal variation.

***Table 10. Trend statistics and overall frequency of compound heat–dry events in Rajshahi Division (1992–2022).***

| ***Metric*** | ***Value*** |
|---|---|
| ***Linear slope*** | *−0.384 events/year* |
| ***Sen's slope*** | *−0.300 events/year* |
| ***MK Z*** | *−2.44* |
| ***p-value*** | *0.0145* |
| ***Kendall's Tau*** | *−0.308* |
| ***Overall event frequency*** | *14.55% of months* |

### 4.5 Change-Point Detection.

#### 4.5.1 Change-Point Detection in Annual Compound Heat–Dry Event Frequency

The annual frequency of compound heat–dry events exhibited a distinct temporal shift during the study period (***Figure 9.***). Event frequency remained comparatively high during the early 1990s, fluctuating between approximately 70 and 90 events per year using ***Eq.3***. Peak frequencies were recorded around 1993–1994, when annual occurrences exceeded 88 events. A rapid decline occurred after the mid-1990s, and event frequency dropped sharply to nearly 40 events around 1998–1999.

Following this transition, annual frequencies remained substantially lower and generally fluctuated between 20 and 45 events throughout the 2000s and 2010s. Several moderate increases were observed around 2005, 2011, and 2015, when frequencies temporarily approached or exceeded 40 events. In contrast, the lowest frequencies occurred after 2018, declining to nearly 15 events around 2020 before showing slight recovery during the final years of the study period. The abrupt reduction in annual event frequency around the late 1990s indicates a notable hydroclimatic transition within the regional climate system.

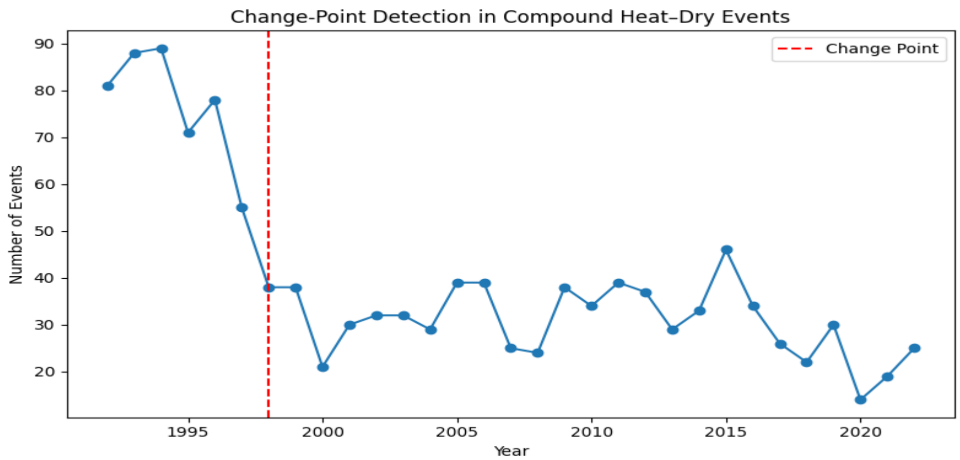


***Figure 9. Change-point detection in annual compound heat–dry event frequency in Rajshahi Division (1992–2022)***

### *4.5.2 Change-Point Detection of Hydroclimatic Regime (1992–2022).*

Pettitt test results identified statistically significant hydroclimatic regime shifts across multiple variables during the study period (***Table 11.***). HDDI recorded a significant change point at index 24 with a p-value of 0.0063. The mean HDDI value shifted from approximately 0.225 before the transition to −0.771 after the shift, indicating a substantial change in hydroclimatic conditions.

Air temperature also exhibited a statistically significant regime shift at index 8 ($p = 0.0081$). Mean air temperature declined from approximately 26.69°C before the shift to 25.56°C afterward, representing a noticeable reduction in regional thermal conditions. Compound heat–dry events showed a moderate shift at index 6 with a p-value of 0.0589. Mean annual event frequency decreased from approximately 23.67 events before the transition to 11.64 events after the shift. These statistical results correspond closely with the temporal variations observed in Figure 4.8, where event frequency and hydroclimatic conditions changed markedly after the late 1990s.

***Table 11. Change-point detection results of hydroclimatic variables using the Pettitt test (1992–2022).***

| *Variable* | *Change Point (Index)* | *p-value* | *Mean Before Shift* | *Mean After Shift* |
|---|---|---|---|---|
| ***HDDI*** | 24 | 0.0063 | 0.225 | −0.771 |
| ***Compound Events*** | 6 | 0.0589 | 23.67 | 11.64 |
| ***Air Temperature*** | 8 | 0.0081 | 26.69°C | 25.56°C |

### *4.6 Spatial Vulnerability Assessment*

District-level vulnerability assessment revealed substantial spatial variability in heat-driven dryness conditions across Rajshahi Division during 1992–2022 (***Table 12.***). Mean HDDI values remained negative for all districts, ranging from approximately −0.0459 in Nawabganj to −0.0777 in Pabna. Compound heat–dry event frequency also varied considerably among districts, with annual event counts ranging from 35 events in Sirajganj to 71 events in Nawabganj.

The calculated Vulnerability Index (***Eq 8.***) showed strong spatial contrasts throughout the division. Nawabganj recorded the highest vulnerability score (1.32), followed by Natore (0.70) and Rajshahi (0.69). Naogaon and Joypurhat also exhibited positive vulnerability values of 0.32 and 0.21, respectively. In contrast, comparatively lower vulnerability conditions were observed in Bogura (−0.62), Pabna (−1.01), and Sirajganj (−1.65). Among all districts, Sirajganj displayed the lowest event frequency and the most negative vulnerability score, whereas Nawabganj experienced both the highest compound event occurrence and the highest vulnerability condition. The spatial differences indicate heterogeneous hydroclimatic exposure across Rajshahi Division during the study period.

| District | HDDI (Mean) | Compound Events | Vulnerability Index |
|---|---|---|---|
| **Bogura** | *-0.0719* | *52* | *-0.62* |
| **Joypurhat** | *-0.0658* | *47* | *0.21* |
| **Naogaon** | *-0.0669* | *55* | *0.32* |
| **Natore** | *-0.0621* | *63* | *0.70* |
| **Nawabganj** | *-0.0459* | *71* | ***1.32*** |
| **Pabna** | *-0.0777* | *40* | *-1.01* |
| **Rajshahi** | *-0.0621* | *59* | *0.69* |
| **Sirajganj** | *-0.0752* | *35* | ***-1.65*** |

***Table 12. District-level HDDI characteristics, compound event frequency, and vulnerability index in Rajshahi Division (1992–2022).***

## *5.Discussion*

The results indicate a clear long-term hydroclimatic transition in Rajshahi Division during 1992–2022, characterized by decreasing thermal conditions and increasing atmospheric moisture and precipitation ***Figure 3 a-d.*** The increase in humidity and rainfall suggests strengthening moisture transport and changing monsoon dynamics over northwestern Bangladesh(Roy & Ghosh, 2013). Similar hydroclimatic changes have been reported in South Asian monsoon regions, where warming oceans and enhanced atmospheric circulation increased regional moisture availability(Biasutti et al., 2022)and seasonal rainfall variability(Annamalai et al., 2013) align with ***Figure 4 a-p***. In Bangladesh, several recent studies also observed increasing rainfall intensity and changing monsoon behavior, particularly after the late 1990s(Ahmed & Kim, 2003). The stronger increase in pre-monsoon and monsoon moisture conditions may be associated with enhanced Bay of Bengal moisture influx(Hossain et al., 2014) and prolonged monsoon persistence. Increased atmospheric moisture can reduce regional dryness through higher cloud formation and greater latent heat exchange. These conditions may influence future agricultural productivity, groundwater recharge, and drought behavior in northwestern Bangladesh. However, increasing moisture variability may also intensify hydroclimatic uncertainty and seasonal instability under future climate change conditions.

The study further revealed that Earth skin temperature decreased more rapidly than near-surface air temperature, indicating important changes in land–atmosphere thermal interactions (***Table 7.***). This finding is strongly supported by the persistent decline in annual and seasonal SATG conditions (***Figures 6 a-d; Table 8.***). A decreasing SATG suggests weakening thermal contrast between the land surface and lower atmosphere. Such conditions often occur when surface sensible heat flux decreases and latent heat flux becomes relatively stronger due to increased soil moisture and atmospheric humidity(Jiang et al., 2022). The concurrent increase in humidity and precipitation observed in this study supports this explanation in (***Figure 3 a-d***). Moist surface conditions generally reduce surface heating because a larger proportion of incoming energy is used for evaporation rather than sensible heating(Xueyuan et al., 2022). Similar land–atmosphere coupling behavior has been identified in monsoon-dominated environments and semi-arid transitional regions. In northwestern Bangladesh, agricultural expansion, irrigation growth, and increased seasonal moisture availability may also contribute to reduced land surface heating(Haque et al., 2026). Therefore, SATG provides important evidence of changing hydroclimatic energy exchange processes in Rajshahi Division.

Strong seasonal hydroclimatic variability was evident throughout the study period (***Figures 6 a-d.***). The pre-monsoon season remained thermally dominant because of intense solar radiation, dry atmospheric conditions, and delayed monsoon onset. Surface temperatures exceeded 33°C during several pre-monsoon years, reflecting strong land-surface heating before the arrival of monsoon rainfall. In contrast, monsoon conditions were characterized by high humidity and substantial rainfall variability. Such seasonal atmospheric instability is common in northwestern Bangladesh because the region lies within a transitional climatic zone between humid monsoon influence and drought-prone inland conditions(Karmakar, 2019). Seasonal SATG decline across all climatic periods further indicates that land–atmosphere thermal coupling changed consistently throughout the year. The strongest SATG decline during monsoon and post-monsoon seasons suggests increasing atmospheric moisture influence over surface thermal conditions. Previous studies in the Barind Tract also reported increasing rainfall irregularity, changing evapotranspiration behavior, and seasonal thermal instability linked with monsoon variability and groundwater conditions(Mou et al., 2022). Therefore, the observed seasonal variability reflects both climatic forcing and regional land-surface responses.

The HDDI analysis demonstrated that heat-driven dryness weakened substantially during recent decades (***Figures7 a-d; Table 9***). Positive HDDI conditions dominated during the early 1990s, whereas negative values became increasingly common after the late 1990s. Similar hydroclimatic transitions have been identified globally in regions where increasing atmospheric moisture partially offset thermal stress(Goswami et al., 2026). The decline in HDDI corresponds closely with increasing humidity and precipitation observed in this study. Reduced thermal contrast and increasing moisture availability likely suppressed heat-driven dryness conditions over time. The decline in compound heat–dry event frequency further supports this interpretation (***Figure 8; Table 10***). Event frequency decreased substantially after the late 1990s, indicating that simultaneous high-temperature and low-moisture conditions became less persistent. In Bangladesh, recent studies and climate assessments also reported shifting drought characteristics and increasing rainfall variability, particularly in northwestern districts(Shahid, 2012). Although drought risk remains important in the Barind region(Mou et al., 2022), the present findings suggest that hydroclimatic stress is evolving toward more moisture-dominated variability rather than persistent extreme dryness. This changing pattern has important implications for regional drought monitoring and climate adaptation planning.

Pettitt test results confirmed that an abrupt hydroclimatic regime shift occurred around the late 1990s and early 2000s (***Table 11; Figure 9***). Significant change points were detected for HDDI, air temperature, and compound heat–dry events, indicating that the regional climate system experienced structural reorganization rather than gradual variability alone. Such hydroclimatic regime shifts are important because they often reflect large-scale atmospheric circulation changes, monsoon variability, and long-term land–atmosphere feedback processes. The spatial vulnerability assessment further demonstrated that hydroclimatic stress was not uniform across Rajshahi Division (***Table 12***). Nawabganj, Natore, and Rajshahi exhibited comparatively higher vulnerability, whereas Sirajganj and Pabna showed lower vulnerability conditions. These differences may be associated with variations in groundwater availability, Barind surface characteristics, irrigation intensity, and local climatic exposure. Similar spatial heterogeneity has been reported in drought-prone regions of northwestern Bangladesh. Overall, this study provides an integrated hydroclimatic assessment framework by combining SATG, HDDI, compound event analysis, change-point detection, and spatial vulnerability assessment within a single regional analysis. The findings may support future climate adaptation planning, drought management, and hydroclimatic monitoring in Bangladesh. Future research should incorporate higher-resolution satellite observations, soil moisture datasets, and climate model projections to better understand future hydroclimatic transitions and compound climate extremes in the region.

## *6.Conclusion*

The study identified a clear hydroclimatic transition in Rajshahi Division during 1992–2022, characterized by decreasing thermal conditions and increasing atmospheric moisture availability. Both air temperature and Earth skin temperature showed declining trends, while humidity and precipitation increased across annual and seasonal scales. Seasonal analysis further demonstrated strong hydroclimatic variability, particularly during the pre-monsoon and monsoon periods. The persistent decline in Surface–Air Temperature Gradient (SATG) indicates weakening land–atmosphere thermal coupling and changing surface energy exchange conditions associated with enhanced moisture availability. Overall, the findings suggest a gradual transition from heat-dry dominance toward increasingly moisture-influenced hydroclimatic conditions in northwestern Bangladesh.

The study also detected an abrupt hydroclimatic regime shift during the late 1990s through Pettitt change-point analysis. Significant shifts were observed in HDDI, air temperature, and compound heat–dry event frequency, indicating structural reorganization of the regional hydroclimatic system. HDDI values shifted from predominantly positive to negative conditions, while compound heat–dry events declined substantially after the transition period. These findings demonstrate that heat-driven dryness conditions became less persistent over time, reflecting evolving regional climate dynamics and changing moisture–temperature interactions across Rajshahi Division.

Spatial vulnerability assessment revealed strong hydroclimatic heterogeneity across the districts of Rajshahi Division. Nawabganj, Natore, and Rajshahi exhibited comparatively higher vulnerability conditions, whereas Sirajganj and Pabna showed relatively lower vulnerability levels. The consistent increase in humidity and precipitation across all seasons further indicates strengthening atmospheric moisture conditions throughout the region. Despite these important findings, several limitations remain. First, the study relied mainly on NASA POWER datasets due to the limited availability of long-term station observations from the Bangladesh Meteorological Department (BMD). Second, the analysis was conducted at district scale, which may not fully capture microclimatic variability and localized land-surface processes. Nevertheless, the study provides an integrated hydroclimatic assessment framework by combining SATG, HDDI, compound event analysis, change-point detection, and spatial vulnerability assessment within a single regional investigation. The findings may support drought monitoring, regional climate adaptation planning, agricultural water management, and future hydroclimatic research in Bangladesh. Future studies should integrate higher-resolution climate datasets, soil moisture observations, and climate model simulations to better evaluate future compound climate extremes and hydroclimatic transitions.

## References


Ahmed, R., & Kim, I.-K. (2003). Patterns of Daily Rainfall in Bangladesh During the Summer Monsoon Season: Case Studies at Three Stations. *Physical Geography - PHYS GEOGR*, *24*. https://doi.org/10.2747/0272-3646.24.4.295

Annamalai, H., Hafner, J., SOORAJ, K., & Pillai, P. (2013). Global Warming Shifts the Monsoon Circulation, Drying South Asia. *Journal of Climate*, *26*. https://doi.org/10.1175/JCLI-D-12-00208.1

Apoorva Bamal, Uddin, M. G., & Agnieszka I. Olbert. (2025). Assessing the impact of hydro-climatic factors on surface water quality: A global review and synthesis. *Journal of Hydrology: Regional Studies*, *61*. https://doi.org/https://doi.org/10.1016/j.ejrh.2025.102677.

Basak, R., & Makin, H. (2025). *Evolving Compound Climate Extremes and Heatwaves in Dhaka Megacity*. https://www.researchgate.net/publication/399139155_Evolving_Compound_Climate_Extremes_and_Heatwaves_in_Dhaka_Megacity

Biasutti, M., Ting, M., & Hill, S. A. (2022). *How the south Asian monsoon is changing in a warming climate*. UNDRR. https://www.preventionweb.net/news/how-south-asian-monsoon-changing-warming-climate

Dey, S., Anderson, P. C., Bukowski, A. L., & Pilinski, M. D. (2025). Investigation of Gas-Surface Interactions and Neutral Atmospheric Properties and Their Impact on Satellite Drag Coefficients. *Earth and Space Science*, *12*(5). https://doi.org/https://doi.org/10.1029/2024EA003998

Duran, I. (2017). *Use of Z Score for the Standardization of Laboratory Results Reporting*. https://doi.org/10.13140/RG.2.2.26975.66726

Ferozur, R. M., Jahan, C. S., Riad Arefin, & Mazumder, Q. H. (2019). Groundwater potentiality study in drought prone barind tract, NW Bangladesh using remote sensing and. *Groundwater for Sustainable Development*, *8*, 205–215. https://doi.org/https://doi.org/10.1016/j.gsd.2018.11.006.

Frédéric Talbot, Sylvain, J.-D., Guillaume Drolet, Poulin, A., Martel, J.-L., & Richard Arsenault. (2025). Assessing hydroclimatic impacts of climate change in snowy catchments using a physically based hydrological model. *Journal of Hydrology: Regional Studies*, *59*. https://doi.org/https://doi.org/10.1016/j.ejrh.2025.102453.

Good, E. (2016). An in situ-based analysis of the relationship between land surface “skin” and screen-level air temperatures: Land Skin-Air Temperature Relationship. *Journal of Geophysical Research: Atmospheres*, *121*. https://doi.org/10.1002/2016JD025318

Goswami, P., Deng, S., Gallant, A., Guntu, R., & Kreibich, H. (2026). *Rethinking Hydroclimatic Extremes: Occurrence of abrupt Drought-to-Heavy-Precipitation transition events*. https://doi.org/10.31223/X56R2M

Haque, M. R., Arman, M., Moniruzzaman, S., Roy, K., & Islam, A. K. M. S. (2026). Spatiotemporal trends and urban-climate interactions of land surface temperature dynamics across Bangladesh. *Anthropocene*, *54*. https://doi.org/https://www.sciencedirect.com/science/article/pii/S2213305426000226

Hossain, M. S., Roy, K., & Datta, D. K. (2014). Spatial and Temporal Variability of Rainfall over the South-West Coast of Bangladesh. *Climate*, *2*, 28–46. https://doi.org/https://doi.org/10.3390/cli2020028

IPCC. (2014). *Climate Change 2014: Impacts, Adaptation, and Vulnerability. Part A: Global and Sectoral Aspects*.

Islam, M. R. (2019). Rainfall in Bangladesh: Is Rainwater Harvesting a Sustainable Approach for Governing Rainwater? *European Journal of Sustainable Development*, *8*. https://doi.org/10.14207/ejsd.2019.v8n5p433

Islam, M. S., Shafiuzzaman, M., & Mahmud, G. (2025). Explainable deep learning for rainfall prediction: A CNN-XGBoost hybrid approach in the northern region of Bangladesh. *Neural Comput & Applic*, *37*. https://doi.org/https://doi.org/10.1007/s00521-025-11646-z

IWMI. (2026). *IWMI in South Asia*. International Water Management Institute. https://www.iwmi.org/where-we-work/south-asia/

Jiang, K., Pan, Z., Pan, F., Wang, J., Han, G., Song, Y., Zhang, Z., Huang, N., Shangqian, M., & Chen, X. (2022). Influence patterns of soil moisture change on surface-air temperature difference under different climatic background. *Science of The Total Environment*, *822*. https://doi.org/10.1016/j.scitotenv.2022.153607

Jingyi Hu, Yang, Z., Hou, C., & Ouyang, W. (2023). Compound risk dynamics of drought by extreme precipitation and temperature events in a semi-arid watershed. *Atmospheric Research*, *281*. https://doi.org/https://doi.org/10.1016/j.atmosres.2022.106474.

Jui, M. J. F., Haque, M., & Billah, M. (2025). A spatiotemporal analysis of four decades of temperature-precipitation interactions and their agricultural consequences in Bangladesh. *Discov Atmos 3*, *36*. https://doi.org/https://doi.org/10.1007/s44292-025-00063-5

Karimzadeh, S., Ahmadi, A., Baldocchi, D., & Fisher, J. (2025). Climate change has increased global evaporative demand except in South Asia. *Communications Earth & Environment*, *6*. https://doi.org/10.1038/s43247-025-02959-x

Karinou, F., Agathangelidis, I., & Cartalis, C. (2025). Assessing the Combined Impact of Land Surface Temperature and Droughts to Heatwaves over Europe Between 2003 and 2023. *Remote Sensing*, *17(9)*(1655). https://doi.org/https://doi.org/10.3390/rs17091655

Karmakar, S. (2019). *PATTERNS OF CLIMATE CHANGE AND ITS IMPACTS IN NORTHWESTERN BANGLADESH*. *48*. https://www.researchgate.net/publication/338172173_PATTERNS_OF_CLIMATE_CHANGE_AND_ITS_IMPACTS_IN_NORTHWESTERN_BANGLADESH

Kendall, M. G. (1975). Rank Correlation Methods. In *Charles Griffin*.

Kim, Y.-S., Kim, M. K., Fu, N., Jiying Liu, Junqi Wang, & Jelena Srebric. (2025). Investigating the impact of data normalization methods on predicting electricity consumption in a building using different artificial neural network models (. *Sustainable Cities and Society*, *118*. https://doi.org/https://doi.org/10.1016/j.scs.2024.105570.

Miah, M., Ullah, S., & Siddique, M. (2022). Heat Waves in Bangladesh: Understanding the Threats and Finding Solutions. *Asia Pacific Journal of Energy and Environment*, *9*. https://doi.org/10.18034/apjee.v9i2.765

Mou, M., Naim, J., & Paul, S. (2022). Climate Change and Groundwater Depletion Induced Agricultural Drought: An Empirical Investigation from Central Barind Tract of Bangladesh. *Rajshahi University Journal of Science*, *9*(18). https://www.researchgate.net/publication/364906075_Climate_Change_and_Groundwater_Depletion_Induced_Agricultural_Drought_An_Empirical_Investigation_from_Central_Barind_Tract_of_Bangladesh

NASA. (2020). *NASA Prediction Of Worldwide Energy Resources (POWER) Data Access Viewer*. https://power.larc.nasa.gov

Pettitt, A. N. (1979). A non-parametric approach to the change-point problem Author: Pettitt, A. N. Journal: Year: 1979 Volume: 28 Issue: 2 Pages: DOI: *Journal of the Royal Statistical Society: Series C (Applied Statistics)*, *28*(2), 126–135. https://doi.org/10.2307/2346729

Rayhan, M., & Rounak Afroz. (2024). , , Evaluating climate models to analyze drought conditions in the western region of Bangladesh ISSN. *Progress in Disaster Science*, *23*. https://doi.org/https://doi.org/10.1016/j.pdisas.2024.100356.

Roy, M., & Ghosh, S. (2013). *RAINFALL VARIATION IN BANGLADESH: TRENDS, FACTORS AND EFFECTS*. https://www.researchgate.net/publication/354161287_RAINFALL_VARIATION_IN_BANGLADESH_TRENDS_FACTORS_AND_EFFECTS

Saira, B. (2023). CLIMATE CHANGE VULNERABILITIES IN SOUTH ASIA: PROSPECTS OF WATER, AGRICULTURE AND FOOD SECURITY. *Russian Law Journal*, *11*. https://www.researchgate.net/publication/393892173_CLIMATE_CHANGE_VULNERABILITIES_IN_SOUTH_ASIA_PROSPECTS_OF_WATER_AGRICULTURE_AND_FOOD_SECURITY

Sarker, T., R., & S., R. (2026). Geospatial mapping of heatwaves and drought: Exploring their link to vegetation, soil moisture, and groundwater in the thirsty Barind Tract, Bangladesh. *Environ Earth Sci 85, 88*. https://doi.org/https://doi.org/10.1007/s12665-025-12787-z

Sen, P. K. (1968). Estimates of the Regression Coefficient Based on Kendall's Tau. *Journal of the American Statistical Association*, *63*(324), 1379–1389. https://doi.org/10.1080/01621459.1968.10480934

Shaha, S. A., & Kiran, M. (2021). MANN-KENDALL TEST: TREND ANALYSIS OF TEMPERATURE, RAINFALL AND DISCHARGE OF GHOTKI FEEDER CANAL IN DISTRICT GHOTKI, SINDH, PAKISTAN. *Environment & Ecosystem Science (EES)*. https://doi.org/DOI: http://doi.org/10.26480/ees.02.2021.137.142

Shahid, S. (2012). Rainfall variability and changes in Bangladesh during the last fifty years. *Rainfall: Behavior, Forecasting and Distribution*. https://www.researchgate.net/publication/286565576_Rainfall_variability_and_changes_in_

Bangladesh_during_the_last_fifty_years

WMO. (2026). *State of the Global Climate 2025*. State of the Global Climate. https://wmo.int/publication-series/state-of-global-climate/state-of-global-climate-2025

Xueyuan, R., Ping, Y., P, Y., X, Y., & Y, Y. (2022). Energy Distribution Characteristics and Environmental Impact Factors in Different Regions of the Summer Monsoon Transition Zone. Front. Environ. Sci. 10:847725. *Frontiers in Environmental Science*, *10*. https://doi.org/10.3389/fenvs.2022.847725

Zhou, S., Wu, S., Gao, J., Liu, L., Li, D., Yan, R., & Wang, J. (2024). Increased stress from compound drought and heat events on vegetation. *Science of The Total Environment*, *949*. https://doi.org/https://doi.org/10.1016/j.scitotenv.2024.175113.

Zscheischler, J., Westra, S., Hurk, B., Seneviratne, S., Ward, P., Pitman, A., AghaKouchak, A., Bresch, D., Leonard, M., Wahl, T., & Zhang, X. (2018). Future climate risk from compound events. *Nature Climate Change*, *8*. https://doi.org/10.1038/s41558-018-0156-3